

Supply-based Feedback Control Strategy of Air-conditioning Systems for Direct Load Control of Buildings Responding to Urgent Requests of Smart Grids

Shengwei Wang and Rui Tang

Department of Building Services Engineering, The Hong Kong Polytechnic University, Kowloon, Hong Kong

Abstract: Power demand response (DR) of buildings is considered as one of most promising solutions to power imbalance and reliability issues in smart grids while demand response control of air-conditioning systems is a most effective means. A fast demand response control strategy, direct load control by shutting down part of operating chillers, has received great attention in recent DR researches and applications. This method, however, would lead to uneven indoor air temperature rises among individual air-conditioned spaces due to the failure of proper distribution of limited cooling supply by the conventional demand-based feedback control strategy commonly used today. A novel supply-based feedback control strategy is therefore proposed to effectively solve the problems caused by the fast demand response and power limiting control strategy. This proposed strategy employs global and local cooling distributors based on adaptive utility function to reset the set-points of chilled water flow and air flow for each zone and space online. Simplified offline and online identification methods, for the two parameters respectively, ensure the convenience and robustness of the adaptive utility function in applications. Case studies are conducted on a simulated air-conditioning system to test and validate the proposed control strategy. Results show that the proposed control strategy is capable not only to maintain even indoor air temperature rises, but also to avoid the operation problems during DR events. Moreover, rather high indoor relative humidity is obviously decreased. The power rebound phenomenon is also relieved and the original comfort control of spaces can be resumed much quickly.

Keywords: fast demand response, smart grid, supply-based feedback control, adaptive utility function, direct load control, building demand management.

The short version of the paper was presented at REM2016 on April 19-21, Maldives. This paper is a substantial extension of the short version

33 **1. Introduction**

34 The power balance between the supply side and the demand side of an electrical
35 grid is a critical issue in the grid operation. However, the rapid growth of electricity
36 demand and the integration of large amounts of renewable generations, which heavily
37 depend on the weather conditions, impose huge stress on balance of electricity grid [1].
38 Any power imbalance can significantly affect the power reliability and quality, and even
39 may lead to the grid failure if the grid balance fails to be recovered on time. Smart grid
40 technology provides a promising solution for enhancing the balance of power grids by
41 improving the ability of electricity producers and consumers to communicate with each
42 other and make decisions about how and when to produce and consume electrical power
43 [2]. The control of power demand at the consumer side in response to grid requests (e.g.,
44 dynamic price and reliability information) is known as demand response (DR). DR
45 program, as one of the most important means in the electrical grid management, has
46 been promoted to encourage the end-users to change their load profiles under a
47 specified pricing policy or request of the grid, which are dynamic or event-driven short-
48 term modifications [3-5]. For instance, some Regional Transmission Operators (RTOs)
49 and Independent System Operators (ISOs), such as Midwest ISO, New York ISO
50 (NYISO) and ISO New England (ISONE), have allowed demand response resources
51 (DRRs) to provide ancillary reserves to maintain the balance of electricity grids [6].

52 Buildings, as the primary energy end-users, could play an important role in power
53 demand response in smart grids. Buildings consumed 74% of electrical energy in the
54 USA [7] and over 90% of the total electricity in Hong Kong [8]. The interaction
55 between buildings and the power grids could be very effective due to elastic nature of
56 building energy use. The building demand management aims at minimizing the impact
57 of peak demand charges and time-of-use rates on the service quality of buildings.
58 Heating, ventilation, and air-conditioning (HVAC) systems, accounting for more than
59 50% of energy demand in buildings, are excellent demand response resources to reduce
60 or shift the electricity demand during peak period, as well as their elastic nature [9]. In

61 residential buildings, most of demand response management is to optimize the schedule
62 of equipment operation to reduce the electricity consumption [10, 11]. In contrast, the
63 control method involved in commercial buildings during peak load period, which not
64 only achieve economic benefits for building owners but also avail to the supply side of
65 electricity grids, is complicated. Load shifting and load shedding are the two major
66 means for peak load management in commercial buildings. Load shedding control
67 reduces peak electric load in a building via turning off non-essential electrical load [12,
68 13].

69 Compared with the load shedding, load shifting which is the process of shifting on-
70 peak load to off-peak hours so as to take advantage of electricity rate difference in
71 different periods is more commonly-used for demand side management in commercial
72 buildings. Four typical categories of facilities are widely used for peak loading shifting,
73 including: building thermal mass (BTM) [14-17], thermal energy storage system (TES)
74 [18-21], combined use BTM with TES [22-24] and phase change materials (PCM) [25-
75 28]. However, due to inevitable energy loss in the charging and discharging processes
76 in peak load shifting, the peak load reduction is realized at the expense of the increased
77 energy consumption. In addition, demand shifting control cannot achieve a significant
78 immediate power reduction with a short time interval (i.e., minutes) resulting from the
79 inherent and significant delay of charge and discharging control processes. This
80 demand response controls, therefore, cannot fulfill the needs of the grid real time
81 operation without any pricing information well in advance.

82 In fact, direct load control by shutting down some of the operating chillers in
83 buildings can achieve immediate demand reduction, which has attracted the increasing
84 attention of users. For example, the utility company (CLP) in Hong Kong has recently
85 launched a pilot demand response programme, namely “Automated DR programme”,
86 which is actually a direct load control program. Shutting down some of chillers by the
87 utility company automatically and remotely when there is an urgent need in power
88 reduction is a major means for the direct load control for commercial buildings [29, 30].
89 However, simply shutting down chillers at the cooling supply side will result in disorder

90 of the entire air-conditioning system control because the control strategies commonly
91 used in centralized air-conditioning systems today are demand-based feedback control
92 [31]. Such demand-based feedback control strategies are based on the assumption that
93 the cooling supply by chillers is set to be enough to fully satisfy the requirements of the
94 terminal units (i.e., AHUs (air handling units)). If the cooling supply is far from
95 sufficient, extremely serious operation problems would be caused, such as excessive
96 speeding of chilled water pumps and air delivery fans, imbalanced chilled water
97 distribution among AHUs, and imbalanced air distribution among VAV (variable air
98 volume) terminals. These would result in very large differences of indoor air
99 temperatures among different air-conditioned spaces and extra power consumption.
100 Such operation problems may also relieve the demand reduction effect of DR control.
101 In addition, the power rebound phenomenon is another serious problem right after DR
102 events. The cooling demand during this period would be very high and individual air-
103 conditioned spaces compete for the cooling supply to push their comfort levels to their
104 original set-points. Thus, all the equipment in the air-conditioning system will be
105 operated at full capacity and a huge stress will be boosted on the electricity grids during
106 power rebound periods.

107 This study therefore addresses the fast demand response by limiting cooling supply
108 directly allowing the commercial buildings to actively and effectively respond to short-
109 term pricing changes or urgent requests from smart grids. In fact, a previous publication
110 of the authors of this article presented a water flow supervisor based on adaptive utility
111 function to effectively solve the problem of disordered water distribution in chilled
112 water system under the reduced cooling supply [32]. However, that publication only
113 addressed the basic concept and approach of supply-based feedback control and
114 demonstrated/testified its application on chilled water systems. The comprehensive
115 concept and common methodology of supply-based feedback control were not
116 established. The general approach of supply-based feedback control for systems of
117 multiple levels was not developed. The generally applicable parameter identification
118 method of the strategy and the control of humidity were not addressed. In this article,

119 these essential aspects are further addressed and developed on the basis of previous
120 work. Firstly, a comprehensive concept of supply-based feedback control strategy and
121 associated common methodology are developed and presented. This control strategy
122 properly controls the distribution of limited cooling supply among users proactively
123 based on the comfort feedback conditions from air-conditioned spaces and provides a
124 solution to the inherent operation problems of commonly-used demand-based feedback
125 control strategies. Secondly, the proposed control strategy employs global and local
126 cooling distributors based on adaptive utility function to reset the set-points of chilled
127 water flow and air flow for each zone and space online while based on the monitored
128 states finally achieved in different zones and spaces to establish the feedback
129 mechanism. Thirdly, the global cooling distributor for chilled water system and the
130 local cooling distributors for air-side systems, for practically realizing the proposed
131 supply-based feedback control for systems of multiple levels, are developed and
132 validated. Furthermore, a simplified practically applicable offline and online
133 identification methods are developed to identify the two parameters of the utility
134 function respectively. Finally, the problem of high indoor relative humidity occurred
135 under limited cooling supply is considered. Case studies are conducted on a simulated
136 air-conditioning system including the water and air sides to test and validate the
137 proposed control strategy. The control performance of the proposed supply-based
138 feedback control strategy is evaluated and compared with that using the conventional
139 demand-based feedback control strategy during a DR event.

140 **2. Problems of conventional demand-based feedback control in DR** 141 **events and concept of proposed supply-based feedback control**

142 Almost all the automatic control strategies commonly-used today for air-
143 conditioning systems in buildings are demand-based feedback control. The control
144 mechanism of typical demand-based feedback control of an air-conditioning system in
145 a building is shown in Fig.1. The regulators, typically PID controllers, modulate the

146 cooling intakes from their suppliers to maintain the states of the spaces served by the
147 terminal units (or states of AHU outlets) at their set-points.

148 The control of cooling distribution in an air-conditioning system is based on the
149 cooling demands of individual air-conditioned spaces, i.e., demand-based feedback
150 control. The cooling generated by chillers is delivered to the cooling demand side (i.e.,
151 indoor spaces) based on their cooling loads. Each AHU and its regulator form a local
152 feedback control loop, which controls the cooling (i.e., chilled water) taken from its
153 supply side (i.e., chillers) based on what needed by the terminal units served by the
154 AHU, typically controlling the supply air temperature at the expected value (i.e., set-
155 point). Such control assumes that all AHUs can get what they need from chillers. In
156 fact, it is the case as the control of chillers is also based on the demands of the AHUs
157 they serve. Similarly, the cooling (i.e., air flow) taken by each terminal unit from its
158 supply side (i.e., AHU) is also based on what needed by space it serves, typically
159 controlling the space air temperature at its set-point. Again, this control is based on the
160 assumption that all terminal units can get what they need from AHUs. The distribution
161 of the cooling in a building is therefore managed based on those standalone demand-
162 based feedback control loops.

163 The distribution of the cooling based on the demand-based feedback control loops
164 can be managed properly in normal conditions while the total demand to each device is
165 not more than what it can provide and all users can get what they need from their
166 suppliers. However, after shutting down some of operating chillers during DR events,
167 the cooling supply is limited and not enough to meet the cooling demand of the building.
168 Serious unbalanced cooling distribution and system operation/control problems would
169 occur both at the water side and the air side of the air-conditioning system. With limited
170 cooling supply, all cooling devices at demand side (e.g., AHUs and VAV boxes) would
171 compete for the limited cooling supply. The modulating valves/dampers of most
172 cooling devices at their demand side will be fully opened quickly as they could not
173 maintain the controlled variables at their set-points. The cooling distributions both
174 among water side users (i.e., individual zones) and air side terminal units (i.e.,

175 individual spaces) will not be evenly reduced, which would lead to the indoor
176 environments in part of zones/spaces sacrificing to unacceptable levels much more
177 quickly than other zones/spaces. The high supply air temperatures of AHUs would also
178 cause the relative humidity in certain spaces beyond the comfortable range seriously.
179 In addition, secondary chilled water pumps at the water side and supply fans at the air
180 side would be operated at full speed. It is due to the need to maintain the preset
181 differential pressure by secondary chilled water pumps and the static pressure by supply
182 fans in the condition of fully opened valves. The excessive speeding of secondary
183 chilled water pumps and air delivery fans would result in significantly increased power
184 consumption and relieve the effects of DR control on power reduction. Furthermore,
185 right after DR events, namely power rebound period, similar operation problems would
186 occur again until the air-conditioning system resumes to the normal condition.

187 A completely new control concept, supply-based feedback control strategy, is
188 proposed to solve the inherent operation problems effectively during DR events and
189 rebound periods as shown in Fig.2. At the chilled water side, the supply-based feedback
190 control (i.e., global cooling distributor) manages the distribution of the total available
191 chilled water (i.e., total cooling supply) among the individual zones based on the
192 measured average space temperatures of all zones aiming at keeping space temperatures
193 of all zones the same (rising gradually during DR events). Similarly, at the air side, the
194 supply-based feedback control (i.e., local cooling distributor) manages the distribution
195 of the total available cooling supply of an AHU among the individual spaces based on
196 the measured space temperatures of all spaces in the zone aiming at keeping
197 temperatures of all spaces the same.

198 Same to the conventional (demand-based) feedback control strategies widely used
199 today, the supply-based control strategy also based on the actual measurements as the
200 feedback to ensure the accuracy, adaptiveness and simplicity of cooling distribution as
201 it is hard for a simple predictive control to achieve the same control performance due
202 to the complexity and every change of conditions and disturbance factors. In fact, major
203 difference compared with the conventional control strategies is that all the feedbacks

204 are from the end-user side (i.e., space indoor temperature) rather than from their
205 immediate outlets (e.g., outlet air temperatures of AHUs).

206 **3. Proposed fast demand response and power limiting control strategy**

207 Compared with traditional power grids, smart grids enable a bidirectional operation
208 (i.e., “two ways” connection with power flow and information flow) to improve power
209 reliability and energy performance. Buildings are the major energy consumers today
210 and their shares are still increasing due to the urbanization. Buildings can benefit power
211 grids by relieving the pressure of power imbalance in different energy processes. Due
212 to the advanced technologies such as building automation systems and smart meters,
213 the demand response control strategies in buildings could be implemented to realize
214 this bidirectional operation mode between power grids and buildings. Fig.3 illustrates
215 the technology infrastructure for implementation of the fast building demand response
216 method supported by the proposed supply-based feedback control, which establishes
217 the communication and interaction between building automation systems of
218 (commercial or non-residential) buildings and smart grids via smart meters. The smart
219 meters are the interface or bridge for the communication between a power grid and
220 buildings to achieve interaction and optimization.

221 When there is an urgent DR request from a smart grid (e.g., sudden price incentive
222 or power reduction request), a fast demand response and power limiting control strategy
223 is proposed to achieve an immediate power reduction by proper control of the air-
224 conditioning systems in buildings. A schematic of the control strategy is shown in Fig.4.
225 Once a DR request is received from the grid, a power demand optimization module,
226 based on the incentive and using the building power demand predictor, determines the
227 power limiting threshold and system alternative settings during the DR event, including
228 the numbers of chillers and secondary pumps to be shut down and fan speeds as well.
229 With the power limiting threshold and instantaneous power demand measured by the
230 power meter, the chiller load regulator fine-tunes the chiller power consumption by
231 adjusting the chilled water flow. The purpose of using this chiller load regulator is to

232 adjust the power consumption of the air-conditioning system allowing the total building
233 power consumption within preset limiting threshold. According to the total cooling that
234 can be delivered to users, cooling distributors are used to distribute the cooling supply
235 using the developed supply-based feedback control strategy instead of conventional
236 demand-based feedback control strategy. At the water side, the global cooling
237 distributor determines the distribution of chilled water to individual AHUs (i.e., zones)
238 based on the measured temperatures of return air to AHUs. At the air side, for each zone,
239 a local cooling distributor is used to determine the distribution of supply air flow to
240 individual VAV boxes (i.e., spaces) based on the measured return air temperatures of
241 the spaces. This paper focuses on the newly proposed supply-based feedback control of
242 air-conditioning systems at both the water and air sides, which solves the inherent
243 problems of conventional demand-based feedback control of air-conditioning systems
244 when the fast demand response and power limiting control strategy is implemented.
245 The development and use of the building power demand predictor [16], power demand
246 optimization [16] and chiller load regulator [33] can be found in previous publications.

247 **4. Cooling distributor based on adaptive utility function**

248 With limited cooling supply in a building when some essential operating chillers
249 are shut down, the cooling distributors are responsible for managing the cooling
250 distribution among individual air-conditioned spaces to realize even reduction of the
251 comfort level. As shown in Fig.2 and Fig.4, a global cooling distributor is employed at
252 the chilled water side while a local cooling distributor is employed at the air side and
253 the working principles of these two cooling distributors are similar. It is worth noticing
254 that more or less levels of cooling distributors could be employed according to the
255 configuration of the air-conditioning system in a building. Fig.5 explains the basic
256 mechanism in managing the distribution among n zones. Generally, n zones should
257 reach a uniform target value of thermal comfort index constrained by the total cooling
258 resource provided. Compared with the target value determined, the cooling allocated to
259 zones (e.g., 1, 2) with lower thermal comfort index should be increased while the

260 cooling allocated to the zones (e.g., n) with higher thermal comfort index should be
 261 reduced. The change of cooling to each zone is determined by the difference between
 262 the target value and the current value of its thermal comfort index (i.e., ΔU). This
 263 process is similar to the resource distribution issue according to one's need with limited
 264 resource based on the utility concept in economic field. "Utility" represents satisfaction
 265 experienced by the consumer of a good. Utility function expresses the utility as a
 266 function of the amount of the resource consumed [34]. This concept is commonly used
 267 in economics field. It is also used in many other areas besides economics. For example,
 268 utility function is widely used in wireless resource management, such as bandwidth
 269 allocation [35, 36]. This concept is also adopted to solve the operation problems in air-
 270 conditioning systems [32].

271 In this study, the utility value is the thermal comfort index and utility function
 272 describes the relationship between the thermal comfort index and the cooling supply
 273 allocated. The cooling distributor based on adaptive utility function is developed to
 274 achieve supply-based feedback control strategy of an air-conditioning system during a
 275 DR period, while adaptive utility function is proposed to update one of the two
 276 parameters of the utility function online for better accuracy and simplicity of parameter
 277 identification.

278 **4.1 Concept of utility value**

279 In this study, the utility value represents the thermal comfort simply represented by
 280 the indoor air temperature, as illustrated in Eq.(1).

$$281 \quad U_i = 1 - \frac{|T_i - T_{set,i}|}{T_{band}} \quad U_i \in [0,1] \quad (1)$$

282 where, U_i is the utility value of i^{th} zone/space, T_i is the measured indoor air
 283 temperature of i^{th} zone/space. $T_{set,i}$ is the reference set-point (i.e., 24°C in this study) of
 284 indoor air temperature which is predefined for normal operation. T_{band} is a very large
 285 deviation between T_i and $T_{set,i}$, which should be large enough to fully cover the whole

286 possible indoor temperature range of spaces during DR events. Its value is set to be
287 10°C in this study.

288 **4.2 Concept of adaptive utility function**

289 The chilled water flow at the water side or air flow at the air side are the allocated
290 resources for each zone or space, and utility function is defined as Eq.(2) [32].

$$291 \quad U_i = -a_i(M_i - M_{set,i})^2 + 1, \quad M_i < M_{set,i} \quad (2)$$

292 where, M_i is the chilled water/air flow rate supplied to i^{th} zone/space. $M_{set,i}$ is a fictitious
293 reference value of the water/air flow rate which is required to maintain the indoor air
294 temperature at its original set-point before DR events but under current cooling load
295 condition. a_i is a parameter representing the thermodynamic characteristics of i^{th} zone/
296 space.

297 In fact, the utility value (i.e., indoor air temperature) is also affected by a few other
298 factors, such as the supply air temperature. However, during a very short time interval,
299 those factors can be considered unchanged and the utility function with fixed
300 parameters correlating the indoor air temperature with chilled water flow or air flow is
301 valid. To allow the use of the utility function over the entire working range during a DR
302 event, one of the two parameters of the utility function is updated online and the
303 adaptive utility function is employed.

304 **4.3 Parameter identification of adaptive utility function**

305 In adaptive utility function, two parameters, $M_{set,i}$ and a_i , are needed to be
306 determined before application. $M_{set,i}$ is identified and updated online and a_i is identified
307 offline prior to application.

308 Offline identification of parameter a_i

309 The parameter a_i for i^{th} zone/space is identified prior to online application.
310 Although ‘ a_i ’ is not a constant coefficient and changes due to the change of cooling
311 load, it has no significant impact on the actual control performance of the water/air flow

312 distribution among individual zones/spaces during DR events. This is because of the
 313 way of using the adaptive utility function (i.e., online updating of the other parameter,
 314 $M_{set,i}$), which is demonstrated in section 6. Therefore, constant values but different for
 315 individual zones/spaces are predefined in this study.

316 In principle, ' a_i ' varies mainly due to the changes of cooling load, which can be
 317 roughly estimated by the chilled water flow or air flow. The identification method
 318 developed in the previous study [32] is not convenient for practical application. A very
 319 simple identification method, therefore, is developed because of the robustness of the
 320 utility function with an inaccurate ' a_i '. Based on the utility function (i.e., Eq.(2)), ' a_i '
 321 can be used to present the change of indoor air temperature corresponding a change of
 322 chilled water flow (or air flow) at current cooling load, as shown in Eq.(3).

$$323 \quad a_i = \frac{\Delta T_i}{10 \times \Delta M_i^2} \quad (3)$$

$$324 \quad \Delta T_i = (T_{out,i} - T_{set,i}) + 5 \quad (4)$$

325 where, ΔT_i is the indoor air temperature rise (stabilized) of i^{th} zone/space when the air-
 326 conditioning system is shut down. ΔM_i is the chilled water flow rate/air flow just
 327 before shutting down the air-conditioning system. To have a better reliability and
 328 simplify the identification process, the system design data are used. For identifying ' a_i ',
 329 when the air-conditioning system is working, the indoor air temperature is assumed to
 330 be its design value. When the air-conditioning system is off, the indoor air temperature
 331 is assumed to be 5°C higher than the design outdoor air temperature ($T_{out,i}$). Then, ΔT_i
 332 can be calculated by Eq.(4).

333 Online parameter identification of $M_{set,i}$

334 Having the parameter " a_i " as a constant, the value of $M_{set,i}$ at current time step k is
 335 determined by the current measured chilled water/air flow rate (M_i^k) and utility value
 336 (U_i^k), as shown in Eq.(5). In practical applications, the field measurements always have
 337 obvious noise and fluctuation. To solve this problem, a simple filter using a forgetting

338 factor is applied to smooth the updated parameter, $M_{set,i}$, as shown in Eq.(6). Having the
 339 updated parameter ($M_{set,i}$), the utility function can be used to estimate the water/air flow
 340 rate needed to achieve any target utility value for a zone/space after rewriting Eq.(2) as
 341 shown in Eq.(7).

$$342 \quad M_{set,i}^k = M_i^k + \sqrt{\frac{1-U_i^k}{a_i}} \quad (5)$$

$$343 \quad M_{set,i}^k = \lambda M_{set,i}^{k-1} + (1-\lambda)M_{set,i}^k \quad (6)$$

$$344 \quad M_{sp,i}^k = M_{set,i}^k - \sqrt{\frac{1-\bar{U}_{sp}^k}{a_i}} \quad (7)$$

345 where, \bar{U}_{sp}^k is the target utility value of all zones/spaces at current time step, which is
 346 the expected utility value if the temperatures of all zones/spaces are controlled to be the
 347 same. λ is the forgetting factor selected to be 0.95 in this study

348 **4.4 Overall procedure of cooling distribution**

349 A global cooling distributor and a few local cooling distributors are developed to
 350 continuously update the set-points of chilled water flows to different zones and air flows
 351 to different spaces within zones, respectively. At each time step, the set-points are reset
 352 aiming at maintaining the same indoor air temperature rise, i.e., the same utility value,
 353 among different zones/spaces, as illustrated in Eq.(8). For the chilled water distribution,
 354 the total chilled water flow distributed is set to be equal to that in the primary loop,
 355 which can fully take advantage of the cooling supply and prevent the deficit flow
 356 problems, as shown in Eq.(9). The water flow rate of each AHU (zone) is controlled at
 357 the given set-point from the global cooling distributor by modulating the flow control
 358 valve based on a feedback (PID) control (see Fig.4). At the air-side, the speed of supply
 359 fan and the total air flow rate are kept at the same as that at the start of DR events, which
 360 can prevent the increased fan power consumption and maintain the relative humidity of
 361 spaces not too high. This also avoids offsetting the power reduction at the water side
 362 during DR events and relieving the effect of DR control. Thus, the air flow distributor
 363 should meet the constraint, that is, the sum of air flow rate distributed to individual

364 spaces should be equal to the total air flow rate to be distributed, as shown in Eq.(10).
 365 The air flows of the VAV boxes are then controlled at their set-points determined by
 366 their local cooling distributors by modulating the air dampers.

$$367 \quad \sum_{i=1}^n (U_i - \bar{U}_i)^2 = 0 \quad (8)$$

$$368 \quad \left| \sum_{i=1}^n M_{sp,w,i} - M_{w,tot} \right| < \varepsilon \quad (9)$$

$$369 \quad \left| \sum_{i=1}^n M_{sp,a,i} - M_{a,tot} \right| < \eta \quad (10)$$

370 where, U_i is the utility value of i^{th} zone/space at a time step. \bar{U}_i is the average utility
 371 of all zones/spaces. n is the total number of zones/spaces. $M_{sp,w,i}$ is the chilled water
 372 flow rate set-point of i^{th} zone at current time step. $M_{w,tot}$ is the total available chilled
 373 water flows in the primary loop. $M_{sp,a,i}$ is the air flow rate set-point of i^{th} space at current
 374 time step. $M_{a,tot}$ is the total air flow to be distributed in a zone. ε , η are the preset
 375 thresholds.

376 4.5 The process of cooling distribution

377 At the start of a time step, the current state variables, including: the indoor air
 378 temperatures of individual zones ($T_{w,i}^k$) and spaces ($T_{a,i}^k$), the water flow of each zone
 379 ($M_{w,i}^k$) and the total water flow provided in the primary loop ($M_{w,tot}^k$) for the global
 380 cooling distributor, the air flow of each space ($M_{a,i}^k$) and the total air flow supply ($M_{a,tot}^k$)
 381 for the local cooling distributors, are collected. Fig.6 shows the computation flow chart
 382 of the local cooling distributor for the air side system in a zone associated with one
 383 AHU. The utility value of each space ($U_{a,i}^k$) is calculated based on the definition (Eq.(1)).
 384 Then, the parameter ($M_{set,i}^k$) of the utility function for each space is updated online using
 385 the current utility value and actual air flow (Eq.(5)), followed by a data filter (Eq.(6)).
 386 The average of the actual utility values of all spaces within the zone is used as the initial
 387 control target value for all spaces and the air flow rate set-point ($M_{sp,a,i}^k$) of each space

388 is determined using the updated utility function (Eq.(7)), which correlates the utility
389 value and air flow rate of the space. Finally, a flow limit check and fine-tune scheme is
390 employed to check whether the sum of the calculated air flow rate set-points ($\sum_{i=1}^n M_{sp,a,i}^k$)
391 is equal to the actual total available air flow rate ($M_{a,tot}^k$). If the $\sum_{i=1}^n M_{sp,a,i}^k$ is not equal to
392 $M_{a,tot}^k$, the target utility value ($\bar{U}_{sp,a}^k$) will be fine-tuned by adding or subtracting a
393 predefined incremental (Δv). The updated target utility value is then used to calculate
394 the air flow set-points again until the difference between the sum of air flow set-points
395 and the actual total flow rate is within a preset threshold (η). The final air flow rate set-
396 point ($M_{sp,a,i}^k$) of each space is then set as the set-point for the air flow control of the
397 VAV box.

398 The computation process of the global cooling distributor for managing the water
399 distribution at the water side is the same, except the measurements ($M_{a,tot}^k, M_{a,i}^k, T_{a,i}^k$) at
400 the air side are replaced by the measurements ($M_{w,tot}^k, M_{w,i}^k, T_{w,i}^k$) at the water side
401 respectively.

402 After DR events, the proposed control strategy is not released until the indoor air
403 temperatures resume to their original set-points. This can maintain the indoor air
404 temperature at nearly same recover speed and particularly avoid the secondary pumps
405 and fans operated at full capacity due to the high cooling demand in rebound period.

406 5 Test platform

407 Computer-based dynamic simulation is adopted, as an effective mean, to test and
408 validate the online control strategies. In this study, a virtual test platform is built to test
409 the proposed fast demand response and power limiting control strategy using dynamic
410 models developed on TRNSYS [37]. This test platform employs detailed physical
411 models including the building envelop and major components (e.g. chillers, pumps,

412 fans, hydraulic network, air ducts, AHUs) of a central air-conditioning system. The
413 dynamic processes of heat transfer, hydraulic characteristics, water flow and air flow
414 balance scheme, energy conservation and controls among the whole system are
415 simulated.

416 The central chiller plant used in the study is a typical primary constant-secondary
417 variable chilled water system. It consists of six identical chillers with rated capacity of
418 4080 kW and two secondary water pumps. The cooling source for the building comes
419 from the chilled water circulating in the AHUs which cooled down the supply air
420 temperature to a predefined set-point. The building is a high-rise building simulated by
421 a multi-zone model (Type 56) in TRNSYS. Six air-conditioned zones with different
422 cooling load profiles in this building cooled by six AHUs are selected to demonstrate
423 the water side cooling distribution and control strategy.

424 Considering the air side, a VAV system in one of the six zones served by one AHU
425 is simulated in detail, which consists of a supply and a return fan with rated capacity 34
426 kW and 32 kW respectively. The VAV system contains eight spaces with different
427 cooling load profiles and air duct resistance is also concerned. The design supply air
428 static pressure is 650 Pa and fresh air flow set-point of this system is set to be a constant
429 value according to the ASHRAE Standard 62.1-2013.

430 The office hour of the building is between 08:00am and 18:00pm and the DR period
431 is two hours between 15:00pm and 17:00pm in a summer day in Hong Kong. The
432 original indoor air temperature set-point in normal condition is set to be 24°C. In the
433 test, there are four operating chillers before the start of the DR event, and two operating
434 chillers are shut down at the start of the DR event and two chillers remain to operate.

435 **6 Results and Discussions**

436 **6.1 The robustness of parameter a_i**

437 Four test cases were conducted to test and validate the impact of parameter a_i on
438 the robustness of the adaptive utility function in online applications. The values of ‘ a_i ’

439 in Case 1 was determined based on the method described a previous study [32]. In Case
440 2, the values were estimated by simplified approach, i.e., using Eq.(3), and the values
441 of a_i in the other two cases were selected to be very different from the relatively accurate
442 values (i.e., identified in Case 1). Because the working mechanism of the cooling
443 distributors for the air side was similar to that for the water side, this case study was
444 carried out at the water side only. The test platform used was described in section 5.
445 The values of ' a_i ' in the four test cases are listed in Table 1.

446 The results of the four test cases are shown in Fig.7. In Case 2, although the values
447 of parameter a_i of some zones were seriously deviated from the estimated values, the
448 controlled indoor air temperatures of the six zones experienced slight different at the
449 start of the DR period, then quickly approached the very similar profiles within very
450 short time and last during the whole DR event. Although the values of ' a_i ' of certain
451 zones had very significant changes, the indoor air temperature profiles in Case 3 and
452 Case 4 were affected noticeably but the differences between the controlled indoor air
453 temperature profiles of different zones were very small and acceptable for practical
454 applications. It can be concluded that the control strategy is not sensitive to the value
455 of parameter a_i due to the use of the adaptive utility function (compensation of updated
456 parameter M_{set}). Therefore, due to the robustness of parameter a_i , it is acceptable to
457 determine the parameter a_i offline using the simplified estimation method for practical
458 applications.

459 **6.2 Test and validation of cooling distributors**

460 The use of cooling distributors for the supply-based feedback control strategy not
461 just effectively solves the unbalanced distribution problems occurred at the water side
462 and air side of an air-conditioning system during DR events, but also achieves further
463 power reduction by diminishing the operation problems of secondary water pumps and
464 air delivery fans. In addition, the power rebound phenomenon right after DR events is
465 also effectively relieved.

466 Test results on the chilled water system

467 Fig.8 shows the comparison among the indoor air temperature profiles of the six
468 zones using the conventional demand-based feedback control and the proposed supply-
469 based feedback control strategies. In Fig.8(a), using the conventional demand-based
470 feedback control, the indoor air temperature profiles of the six zones are obviously
471 different not only during the DR event, but also right after the DR event. This was
472 mainly because right after the DR event, the cooling demand was very high and
473 individual zones competed for the chilled water again to push their comfort levels back
474 to their original set-points. If the proposed control was released right after the DR event
475 and the conventional control strategy was resumed accordingly, the unbalanced indoor
476 air temperature rises among individual zones would happen again.

477 In Fig.8(b), it can be observed that the temperature profiles of the six zones are
478 almost the same during the DR event using the proposed control strategy when the
479 cooling supply from chillers is limited and have the similar resume profiles after the
480 DR event. The indoor air temperature at 16:00pm had an obvious jump because there
481 was a significant step change introduced on the solar radiation at 16:00pm. This can
482 demonstrate the robustness of proposed control strategy based on adaptive utility
483 function when facing sudden significant changes of cooling loads. After the
484 conventional feedback control was resumed when the indoor air temperature
485 approached their original set-points, the profiles experienced a little differences among
486 individual zones as the results of the handover between the control strategies.

487 Fig.9 presents the actual chilled water flow rates distributed to six individual AHUs
488 using the conventional demand-based feedback control and the supply-based feedback
489 control strategies. During and right after the DR event, the proposed supply-based
490 control strategy achieved stable and proper chilled water distribution among six zones,
491 avoided the disordered water flow distribution effectively and maintained the same
492 indoor air temperature profiles among different zones, as shown in Fig.8(b). In Fig.9(a),
493 using the conventional control strategy, the water flow rates were very high and out of
494 control due to the competition among the zones. Fig.10 shows the chilled water flows
495 in the by-pass line using the conventional demand-based feedback control and the

496 proposed supply-based feedback control strategies. The proposed control strategy could
497 eliminate the deficit flow and keep the water flow rate in the by-pass line about zero
498 during the DR event while there was serious deficit flow when using the conventional
499 strategies.

500 Test results on air-side system

501 Fig.11 shows the indoor air temperature profiles of eight spaces using the
502 conventional demand-based feedback control and the proposed supply-based feedback
503 control strategies. In Fig.11(a), the indoor air temperature profiles of the eight spaces
504 were obviously different both during and right after the DR event. This was mainly
505 because the cooling demand was very high right after the DR event and the individual
506 spaces would compete for the air flow again after the DR event to push their comfort
507 levels back to their original set-points. When the proposed control strategy was adopted,
508 the temperature profiles of the eight spaces were almost the same during the DR event
509 with the limited cooling supply from chillers and also had a similar resume profiles
510 after the DR event, as shown in Fig.11(b). The slight fluctuation was caused by
511 handover between the control strategies after the indoor air temperatures of eight spaces
512 resumed to their original set-points.

513 Fig.12 shows a comparison of the indoor relative humidity of the eight spaces using
514 the conventional demand-based feedback control and the supply-based feedback
515 control strategies. During the DR event, using the conventional control, the relative
516 humidity of these spaces increased seriously and the maximum value reached nearly
517 83%, which was much higher than the acceptable range of indoor air relative humidity.
518 Moreover, the significant differences among spaces were primarily caused by the
519 unbalanced air flow distribution. Although the relative humidity was not the main
520 control objective of the proposed control strategy, the relative humidity of spaces did
521 not increase as high as that using the conventional control, and amounts of increase in
522 some spaces were over 10% less (i.e., reduced from 83% to 72%). It was benefited from
523 the supply fans control. During the DR event, the supply fan was set to be nearly the

524 same speed as that right before the DR event instead of running at full speed. In this
525 case, the supply air temperature would not increase so high due to the decreased total
526 air flow rate by limiting the speed of the supply fan. The control strategy was not
527 switched to the conventional control strategy until the indoor air temperatures of spaces
528 got right. Fig.13 presents the air flow rates distributed to individual spaces using the
529 conventional demand-based feedback control and the supply-based feedback control
530 strategies. During and right after the DR event, the proposed supply-based control
531 strategy achieved stable and proper air flow distribution among eight spaces, avoided
532 the disordered air flow distribution effectively and maintained the same indoor air
533 temperature profiles among different spaces, as shown in Fig.11(b).

534 Power consumption of the air-conditioning system

535 The primary objective of the DR control is to achieve power reduction as much as
536 possible. Shutting down some of the operating chillers directly might be failure to
537 realize a fast power reduction if the whole air-conditioning system is still controlled by
538 the conventional demand-based feedback control strategies. Fig.14 compares the total
539 power consumptions using the two control strategies, including the chillers, the
540 (primary and secondary) water pumps and the (supply and return) fans. It can be
541 observed that, using the conventional demand-based feedback control, the extra power
542 consumption caused by full speed operation of the secondary pumps and fans almost
543 offsets the effect of shutting down chillers. This phenomenon was more seriously
544 compared with the result presented in the previous publication of the authors [32] since
545 only the power effect of full speed operation of secondary pumps (excluding the fans
546 in air-side) was considered there. During the DR event, the proposed control strategy
547 could achieve a power reduction about 1200 kW, accounting for 24% of the power
548 consumption compared with that right before the start of the DR event, while there was
549 almost no power reduction (even increased) due to the compensation of increased
550 power consumption of pumps and fans when using the conventional demand-based
551 feedback control strategies. In addition, it is worth noticing that an obvious rebound
552 phenomenon can be observed after the DR event when the conventional demand-based

553 feedback control strategy was used. Right after the DR event, the cooling demand was
554 very high as individual zones/spaces competed for the provided cooling again to push
555 their comfort levels back to their original set-points. The proposed power limiting
556 control strategy was used during and after the DR event until the indoor air temperatures
557 of all zones/spaces reached their original set-points. Besides, the number of chillers (i.e.,
558 four) was resumed to be the same as that right before the DR event, instead of all chillers.
559 As a result, the power rebound was reduced by a significant amount, i.e., about 3600kW,
560 which was 35.4% of the original total power consumption during the rebound period.

561 **7 Conclusions**

562 A fast demand response and power limiting control strategy is developed which
563 achieves fast power reduction by shutting down some of the chillers directly. A novel
564 control concept, cooling supply-based feedback control strategy, employing global and
565 local cooling distributors based on adaptive utility function, is proposed to properly
566 distribute the chilled water/air flow among different zones/spaces to maintain uniform
567 thermal comfort sacrifice during DR events, instead of the commonly-used demand-
568 based feedback control strategies.

569 Test results show that the proposed cooling supply-based feedback control strategy
570 can facilitate the expected fast demand response and power limiting control strategies
571 to achieve fast power reduction when receiving the demand response requests from
572 smart grids. The proposed control strategy can effectively solve the disordered cooling
573 distribution problem and achieve the uniform reduction profiles of the thermal comfort
574 among different zones/spaces under limited cooling supply. In addition, the associated
575 operation problems of using the conventional demand-based feedback control strategies,
576 such as deficit flow and excessive speeding of secondary pumps and fans, are avoided.
577 The increase of relative humidity is also alleviated during DR events. With the support
578 of the proposed control strategy, the DR control strategy could achieve a significant
579 power reduction, i.e., 24% of the power consumption with acceptable thermal comfort
580 sacrifice. Furthermore, the use of the proposed strategy could significantly reduce the

581 level of the power rebound after DR events and allow the air-conditioning systems to
582 resume normal operation/control much quickly.

583 **8 Acknowledgements**

584 The research presented in this paper is financially supported by a grant (152152/15E)
585 of the Research Grant Council (RGC) of the Hong Kong SAR.

586 **9 References**

- 587 [1] Agency IE. IEA Statistics: World Energy Statistice and Balances: Organisation for Economic
588 Co-operation and Development, International Energy Agency; 1989.
- 589 [2] Yuan J, Hu Z. Low carbon electricity development in China—An IRSP perspective based on
590 Super Smart Grid. *Renewable and Sustainable Energy Reviews*. 2011;15:2707-13.
- 591 [3] Pinson P, Madsen H. Benefits and challenges of electrical demand response: A critical review.
592 *Renewable and Sustainable Energy Reviews*. 2014;39:686-99.
- 593 [4] Wang SW, Xue X, Yan CC. Building power demand response methods toward smart grid.
594 *HVAC&R Research*. 2014;20:665-87.
- 595 [5] Chakraborty A, Ilic MD. Control and optimization methods for electric smart grids: Springer;
596 2012.
- 597 [6] Chen Y, Li J. Comparison of security constrained economic dispatch formulations to incorporate
598 reliability standards on demand response resources into Midwest ISO co-optimized energy and
599 ancillary service market. *Electric Power Systems Research*. 2011;81:1786-95.
- 600 [7] DoE U. Buildings energy databook. Energy Efficiency & Renewable Energy Department. 2011.
- 601 [8] Electrical and Mechanical Services Department of Hong Kong. Hong Kong Energy End-use
602 Data. <www.emsd.gov.hk/emsd/e_download/pee/HKKEUD2012.pdf>. 2012.
- 603 [9] DOE. 2011 DOE Building Energy Data Book, March 2012. <<http://buildingsdatabook.eren.doe.gov/>>. 2011.
- 604 [10] Toronto hydro electric system peaksaver. <<http://www.torontohydro.com/peaksaver>>. 2010.
- 605 [11] Yoon JH, Bladick R, Novoselac A. Demand response for residential buildings based on dynamic
606 price of electricity. *Energy and Buildings*. 2014;80:531-41.
- 607 [12] Grondzik WT, Kwok AG. Mechanical and electrical equipment for buildings: John wiley &
608 sons; 2014.
- 609 [13] Wei M, Houser KW, Orland B, Lang DH, Ram N, Sliwinski MJ, et al. Field study of office
610 worker responses to fluorescent lighting of different CCT and lumen output. *Journal of*
611 *Environmental Psychology*. 2014;39:62-76.
- 612 [14] Herter K, McAuliffe P, Rosenfeld A. An exploratory analysis of California residential customer
613 response to critical peak pricing of electricity. *Energy*. 2007;32:25-34.
- 614 [15] Xu P, Haves P, Piette MA, Braun J. Peak demand reduction from pre-cooling with zone
615 temperature reset in an office building. Lawrence Berkeley National Laboratory. 2004.
- 616 [16] Xue X, Wang SW, Sun YJ, Xiao F. An interactive building power demand management strategy
617 for facilitating smart grid optimization. *Applied Energy*. 2014;116:297-310.
- 618 [17] Kirby B, Kueck J, Laughner T, Morris K. Spinning reserve from hotel load response. The
619

620 Electricity Journal. 2008;21:59-66.

621 [18] Fukai J, Hamada Y, Morozumi Y, Miyatake O. Improvement of thermal characteristics of latent
622 heat thermal energy storage units using carbon-fiber brushes: experiments and modeling.
623 International Journal of Heat and Mass Transfer. 2003;46:4513-25.

624 [19] Kousksou T, El Rhafiki T, El Omari K, Zeraouli Y, Le Guer Y. Forced convective heat transfer
625 in supercooled phase-change material suspensions with stochastic crystallization. international
626 journal of refrigeration. 2010;33:1569-82.

627 [20] Sharma A, Tyagi V, Chen C, Buddhi D. Review on thermal energy storage with phase change
628 materials and applications. Renewable and Sustainable energy reviews. 2009;13:318-45.

629 [21] Kuznik F, David D, Johannes K, Roux J-J. A review on phase change materials integrated in
630 building walls. Renewable and Sustainable Energy Reviews. 2011;15:379-91.

631 [22] Henze GP, Felsmann C, Knabe G. Evaluation of optimal control for active and passive building
632 thermal storage. International Journal of Thermal Sciences. 2004;43:173-83.

633 [23] Hajjah A, Krarti M. Optimal control of building storage systems using both ice storage and
634 thermal mass–Part I: Simulation environment. Energy Conversion and Management. 2012;64:499-
635 508.

636 [24] Hajjah A, Krarti M. Optimal controls of building storage systems using both ice storage and
637 thermal mass–Part II: Parametric analysis. Energy Conversion and Management. 2012;64:509-15.

638 [25] Bentz DP, Turpin R. Potential applications of phase change materials in concrete technology.
639 Cement and Concrete Composites. 2007;29:527-32.

640 [26] Tyagi V, Kaushik S, Tyagi S, Akiyama T. Development of phase change materials based
641 microencapsulated technology for buildings: a review. Renewable and Sustainable Energy Reviews.
642 2011;15:1373-91.

643 [27] de Gracia A, Navarro L, Castell A, Ruiz-Pardo Á, Álvarez S, Cabeza LF. Thermal analysis of
644 a ventilated facade with PCM for cooling applications. Energy and Buildings. 2013;65:508-15.

645 [28] Zhu N, Wang SW, Xu XH, Ma ZJ. A simplified dynamic model of building structures integrated
646 with shaped-stabilized phase change materials. International Journal of Thermal Sciences.
647 2010;49:1722-31.

648 [29] Shan K, Wang SW, Yan CC, Xiao F. Building demand response and control methods for smart
649 grids: A review. Science and Technology for the Built Environment. 2016:00-10.

650 [30] CLP. CLP information kit. [https://www.clpgroup.com/en/Investors-Information-site/
651 Financial%20Reports%20%20Document/2013E109.pdf](https://www.clpgroup.com/en/Investors-Information-site/Financial%20Reports%20%20Document/2013E109.pdf). 2014.

652 [31] Xue X, Wang SW, Yan CC, Cui BR. A fast chiller power demand response control strategy for
653 buildings connected to smart grid. Applied Energy. 2015;137:77-87.

654 [32] Tang R, Wang SW, Gao DC, Shan K. A Power Limiting Control Strategy Based on Adaptive
655 Utility Function for Fast Demand Response of Buildings in Smart Grids. Science and Technology
656 for the Built Environment. 2016, 22(6): 810-819.

657 [33] Cui BR, Gao D-c, Wang SW, Xue X. Effectiveness and life-cycle cost-benefit analysis of active
658 cold storages for building demand management for smart grid applications. Applied Energy.
659 2015;147:523-35.

660 [34] Varian HR. Microeconomic analysis. 1992.

661 [35] Kuo W-H, Liao W. Utility-based resource allocation in wireless networks. Wireless
662 Communications, IEEE Transactions on. 2007;6:3600-6.

663 [36] Kalyanasundaram S, Chong EK, Shroff NB. Optimal resource allocation in multi-class

664 networks with user-specified utility functions. *Computer Networks*. 2002;38:613-30.
665 [37] Wang SW. Dynamic simulation of a building central chilling system and evaluation of EMCS
666 on-line control strategies. *Building and Environment*. 1998;33:1-20.
667

668 **Nomenclature**

669	DR	demand response
670	BTM	building thermal mass
671	TES	thermal energy storage
672	PCM	phase change material
673	AHU	air handling unit
674	VAV	variable air volume
675	U	utility value
676	M	flow
677	T	temperature
678	R	cooling resource
679	n	total number of zones/spaces

680

681 *Greek symbols*

682	λ	forgetting factor
683	ε	preset threshold
684	η	preset threshold

685

686 *Superscripts*

687	k	number of iteration
-----	-----	---------------------

688

689 *Subscripts*

690	sp	set-point
691	tot	total
692	w	water
693	a	air
694	i	i^{th} zone/space
695	out	outdoor

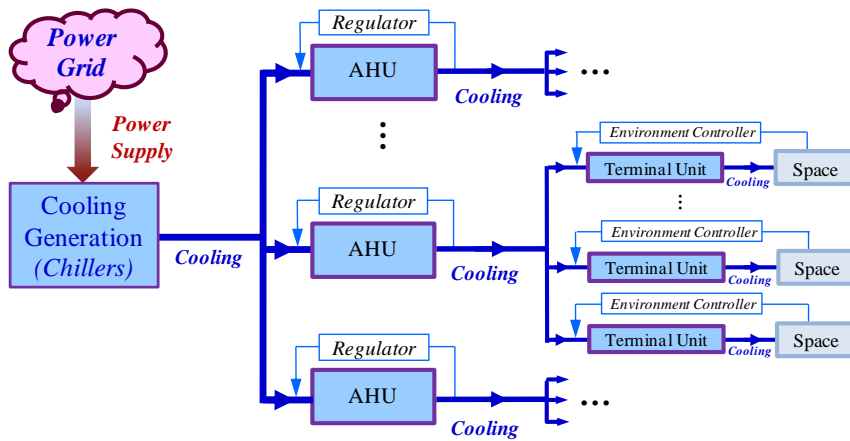


Fig.1. Basic principle of demand-based feedback control

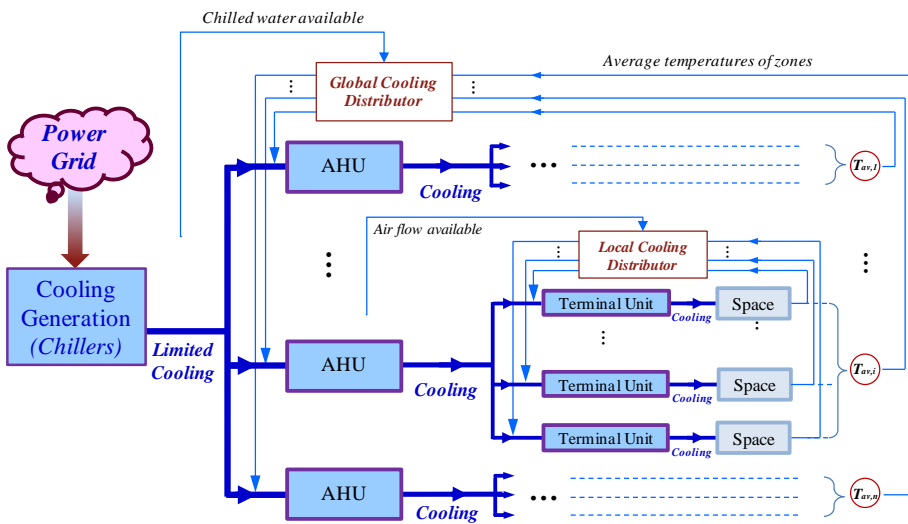


Fig.2 Basic principle of supply-based feedback control

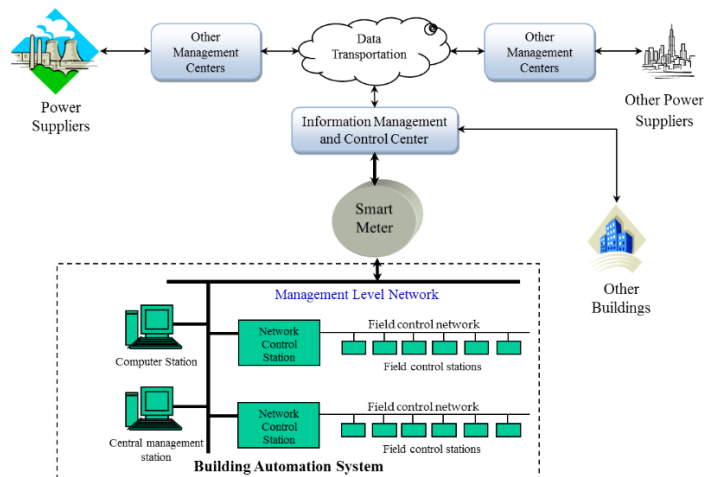


Fig.3 Implementation infrastructure of demand response control strategy

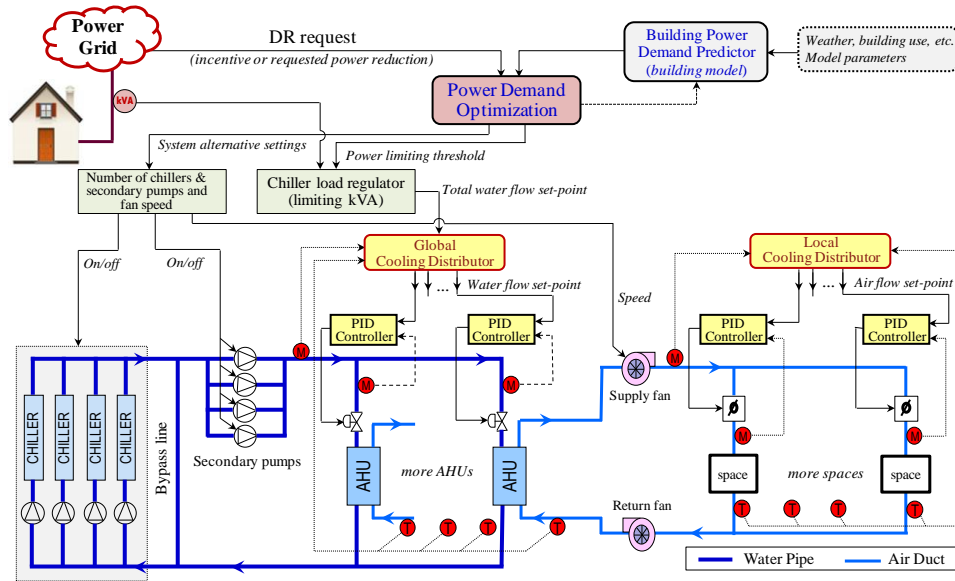


Fig.4 Schematic of fast demand response and power limiting control strategy for air-conditioning systems

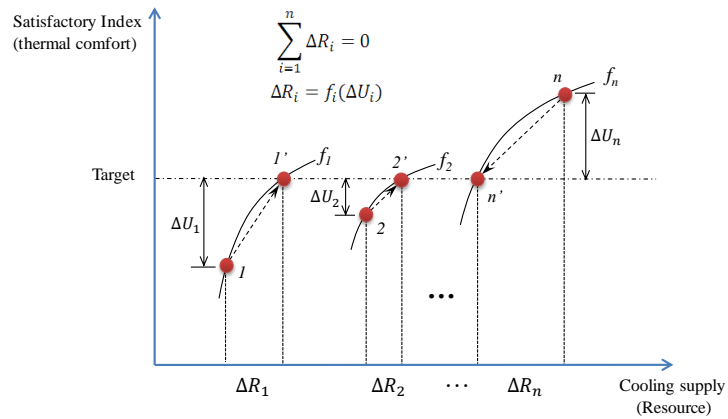


Fig.5 The basic working principle of cooling distributor

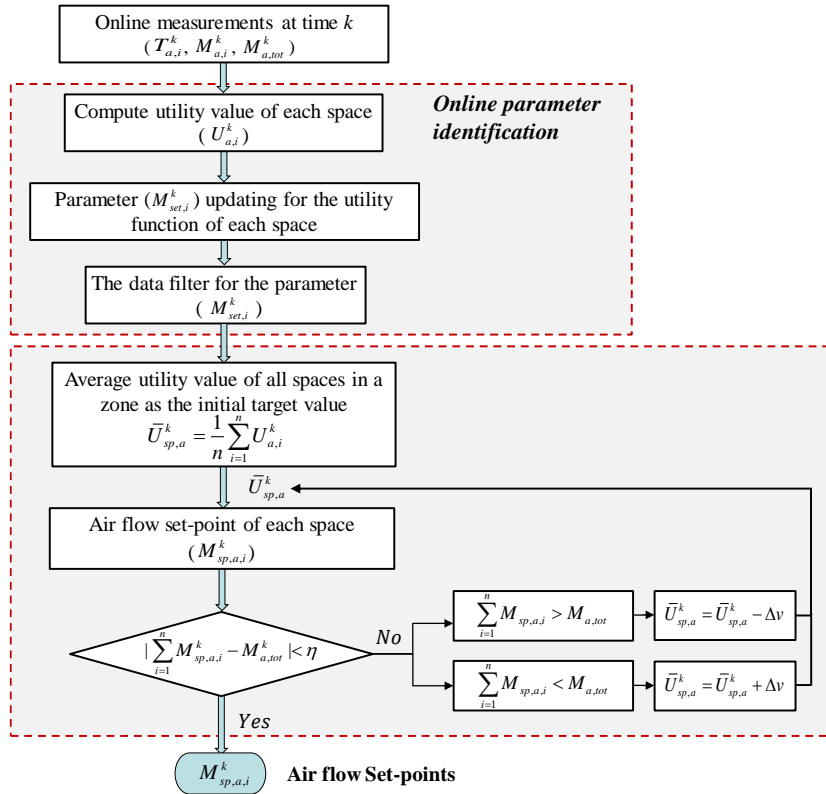


Fig.6 Flow chart of online air flow rate set-point reset scheme of local cooling distributor

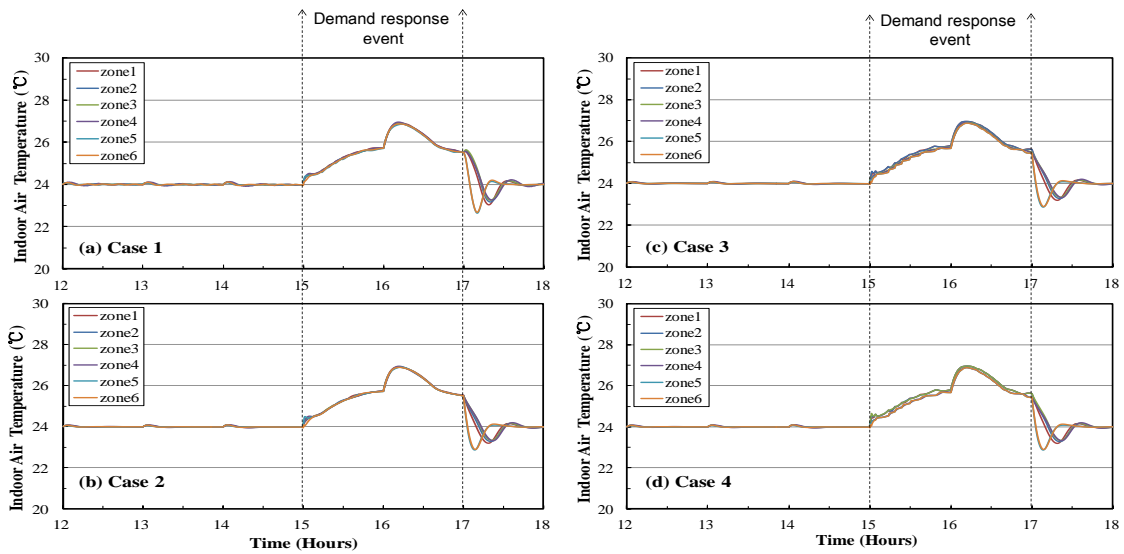


Fig.7 Indoor temperature profiles of four test cases using different values of a_i

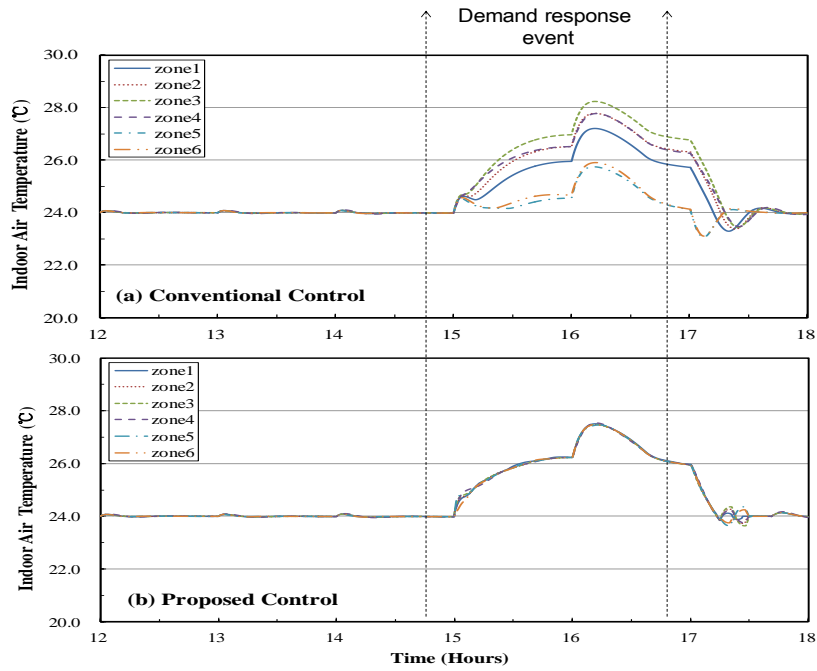


Fig.8 Indoor air temperature profiles of zones in DR tests using conventional and proposed strategies

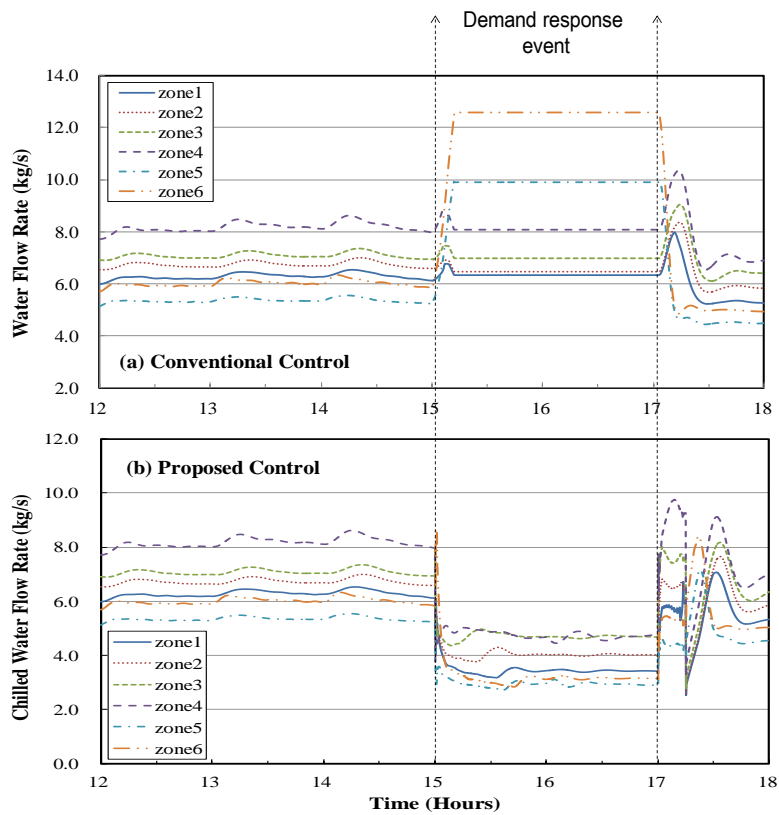


Fig.9 Chilled water flow profiles of zones in DR tests using conventional and proposed strategies

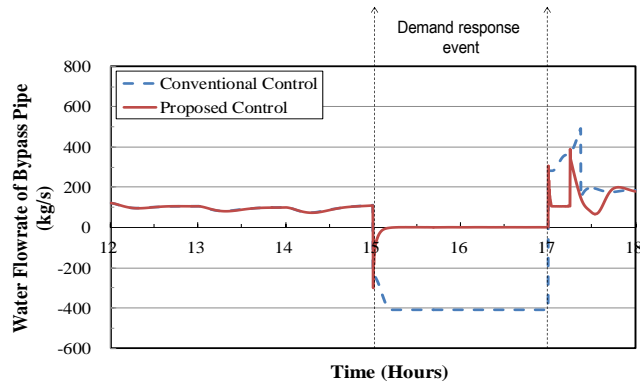


Fig.10 Water flow rates in by-pass line in DR tests using conventional and proposed strategies

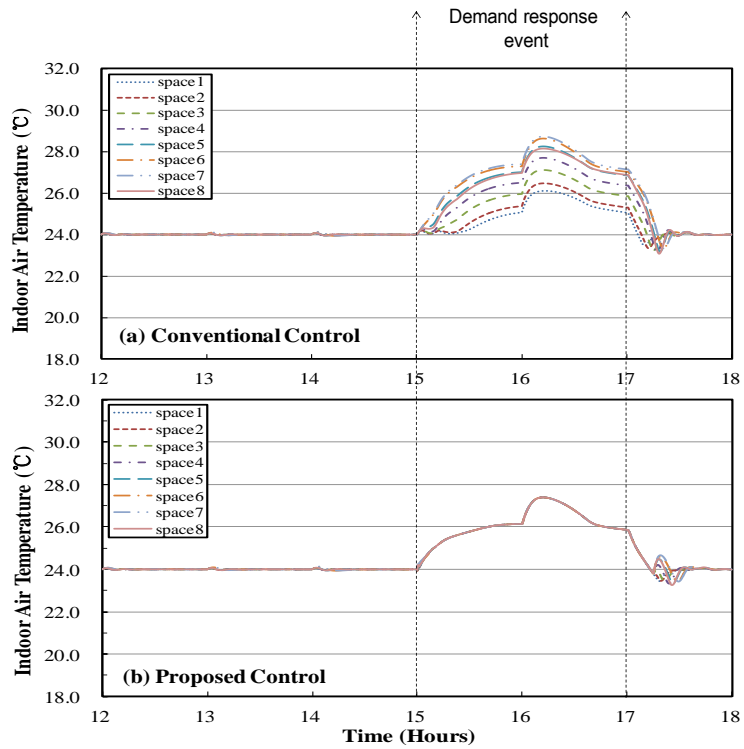


Fig.11 Indoor air temperature profiles of spaces in DR tests using conventional and proposed strategies

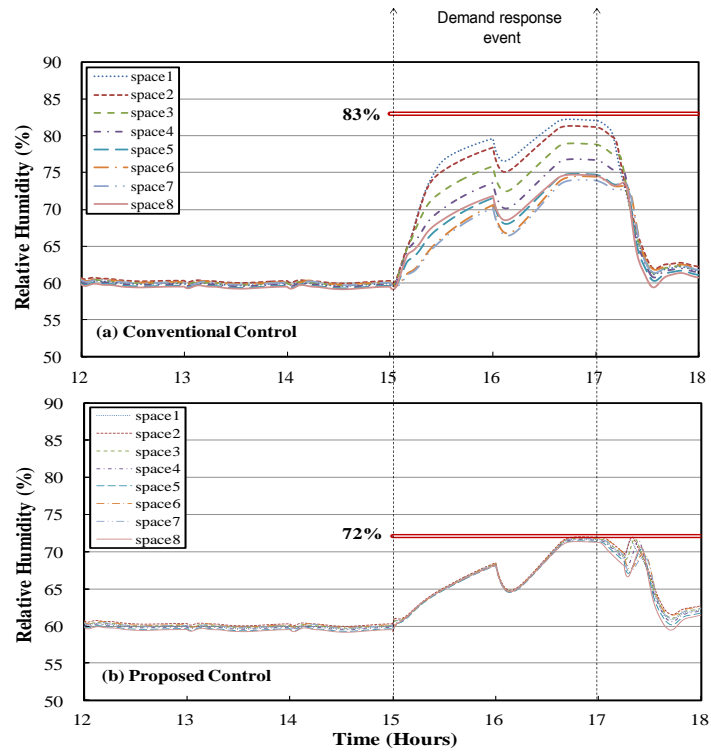


Fig.12 Indoor relative humidity profiles of spaces in DR tests using conventional and proposed strategies

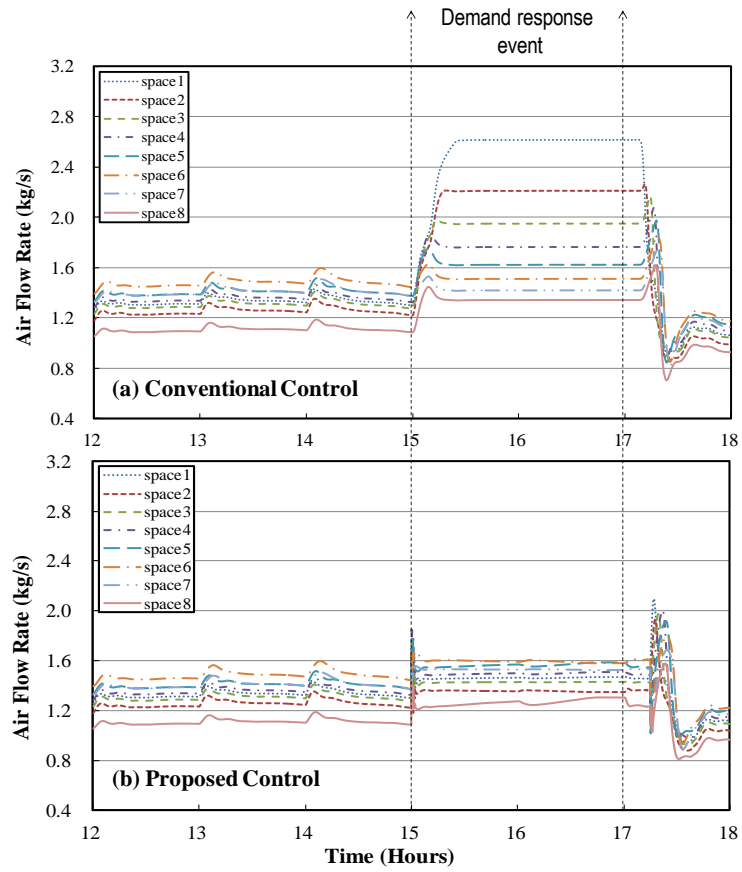


Fig.13 Air flow profiles of spaces in DR tests using conventional and proposed strategies

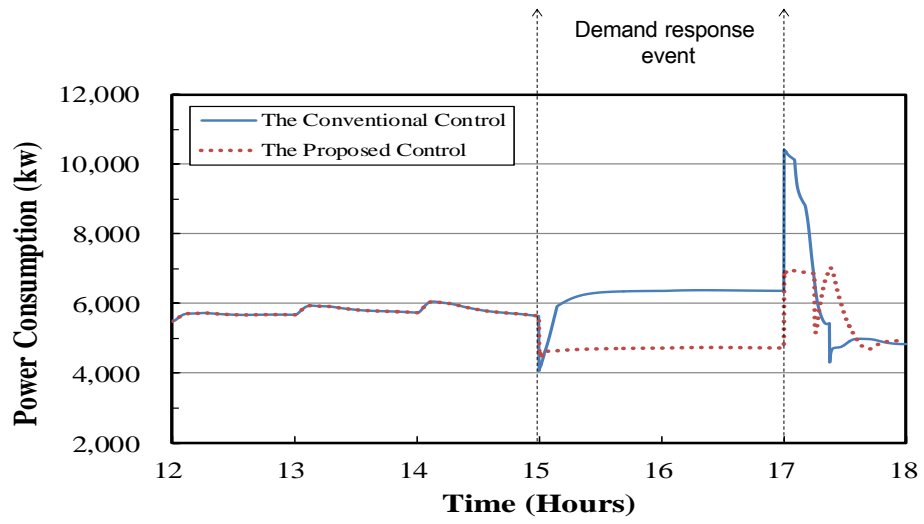


Fig.14 Power consumptions of chiller plant in DR tests using conventional and proposed strategies